

INFORMATION TO USERS

This material was produced from a microfilm copy of the original document. While the most advanced technological means to photograph and reproduce this document have been used, the quality is heavily dependent upon the quality of the original submitted.

The following explanation of techniques is provided to help you understand markings or patterns which may appear on this reproduction.

1. The sign or "target" for pages apparently lacking from the document photographed is "Missing Page(s)". If it was possible to obtain the missing page(s) or section, they are spliced into the film along with adjacent pages. This may have necessitated cutting thru an image and duplicating adjacent pages to insure you complete continuity.
2. When an image on the film is obliterated with a large round black mark, it is an indication that the photographer suspected that the copy may have moved during exposure and thus cause a blurred image. You will find a good image of the page in the adjacent frame.
3. When a map, drawing or chart, etc., was part of the material being photographed the photographer followed a definite method in "sectioning" the material. It is customary to begin photoing at the upper left hand corner of a large sheet and to continue photoing from left to right in equal sections with a small overlap. If necessary, sectioning is continued again -- beginning below the first row and continuing on until complete.
4. The majority of users indicate that the textual content is of greatest value, however, a somewhat higher quality reproduction could be made from "photographs" if essential to the understanding of the dissertation. Silver prints of "photographs" may be ordered at additional charge by writing the Order Department, giving the catalog number, title, author and specific pages you wish reproduced.
5. PLEASE NOTE: Some pages may have indistinct print. Filmed as received.

Xerox University Microfilms

300 North Zeeb Road
Ann Arbor, Michigan 48106

74-6982

RIMMER, Daniel Porter, 1945-
MOLECULAR DIFFUSION IN QUARternary LIQUID
SYSTEMS.

The University of Oklahoma, Ph.D., 1973
Engineering, chemical

University Microfilms, A XEROX Company, Ann Arbor, Michigan

THE UNIVERSITY OF OKLAHOMA
GRADUATE COLLEGE

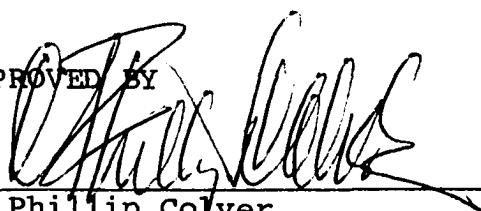
MOLECULAR DIFFUSION IN QUARTERNARY
LIQUID SYSTEMS


A DISSERTATION
SUBMITTED TO THE GRADUATE FACULTY
in partial fulfillment of the requirements for the
degree of
DOCTOR OF PHILOSOPHY

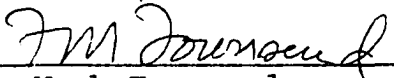
BY
DANIEL PORTER RIMMER
Norman, Oklahoma
1973


MOLECULAR DIFFUSION IN QUARTERNARY
LIQUID SYSTEMS

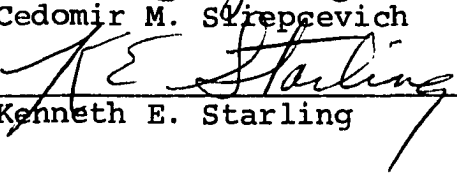
APPROVED BY


C. Phillip Colver


Tom J. Love


F. Mark Townsend


Cedomir M. Srepcевич


Kenneth E. Starling

ACKNOWLEDGEMENTS

The author would like to express his gratitude to Dr. C. P. Colver for his guidance and encouragement throughout the course of this work. Appreciation is extended to Dr. T.J. Love, Dr. F. M. Townsend, Dr. C. M. Sliepcevich, and Dr. K. E. Starling for serving on my advisory committee.

The various contributions of my colleagues Dr. C. J. Vadovic and Dr. K. E. Sanders are gratefully acknowledged.

The author wishes to acknowledge the financial support provided by the following organizations: Dow Chemical Company, Phillips Petroleum Company, Texaco, Continental Oil Company and the National Defense Education Act. Thanks are also extended to Phillips Petroleum Company for donating the chemicals used in this research.

The author expresses gratitude to Miss Margaret Williford and to Miss Nancy Gober for their able assistance in the preparation of this manuscript.

Finally, I wish to express my deepest appreciation to my family for their support and encouragement throughout my education, and especially to my wife, Kathy, for her love and understanding.

ABSTRACT

An experimental technique was developed which allowed the first successful determination of molecular diffusion coefficients in a four component liquid system. The principal components of the diffusion apparatus consisted of a flowing junction test cell, a double Savart plate birefringent interferometer, and a constant temperature air bath. Diffusion coefficients were measured at 25°C for the quaternary system composed of cyclohexane, toluene, n-heptane and n-decane. For this system, the main diffusion coefficients were found to be approximately an order of magnitude greater than the cross diffusion coefficients. An average error of approximately five percent was determined for the main diffusion coefficients.

Expressions were also developed for the prediction of multicomponent diffusivities in liquid systems. The predictive technique was based on the Enskog theory of transport in a dense rigid sphere fluid. This theory, in conjunction with a continuous association model, allowed the prediction of multicomponent diffusivities based upon infinite dilution diffusion data. Diffusivities predicted agreed moderately well with experimental data for three systems.

TABLE OF CONTENTS

	Page
LIST OF TABLES	vi
LIST OF ILLUSTRATIONS	vii
Chapter	
I. INTRODUCTION	1
II. EXPERIMENTAL INVESTIGATIONS	6
III. PREDICTION OF MULTICOMPONENT DIFFUSION COEFFICIENTS	37
IV. CONCLUSIONS AND RECOMMENDATIONS	52
LITERATURE CITED	54
NOMENCLATURE	58
APPENDICES	
A. SOLUTION OF DIFFERENTIAL EQUATIONS FOR MULTICOMPONENT DIFFUSION	60
B. CHEMICAL SPECIFICATIONS	64
C. BINARY DATA ANALYSIS	65
D. LEAST SQUARES ANALYSIS	69

LIST OF TABLES

Table	Page
1. Molecular Diffusion Coefficients at 25°C for the System Cyclohexane (1) - Toluene (2) - n-Heptane (3) - n-Decane (4).	31
2. Comparison of Experimental Main Diffusion Coefficients with Predicted Values.	33
3. Binary Infinite Dilution Diffusion Data at 25°C.	36
4. Comparison of Main Diffusion Coefficients for the System Cyclohexane (1) - Toluene (2) - n-Heptane (3) - n-Decane (4) with Predicted Values.	49
5. Comparison of Experimental Diffusion Coefficients for the System Methanol (1) - Iso-Butanol (2) - n-Propanol (3) with Predicted Values.	50
6. Comparison of Experimental Diffusion Coefficients for the System Acetone (1) - Benzene (2) - Carbon-Tetrachloride (3) with Predicted Values.	51

LIST OF ILLUSTRATIONS

Figure	Page
1. Flowing Junction Test Cell.	10
2. Interferometer Optical Arrangement.	12
3. Photographs of Initial Interface and Interference Patterns	21

MOLECULAR DIFFUSION IN QUARTERNARY
LIQUID SYSTEMS

CHAPTER 1

INTRODUCTION

The study of molecular diffusion in multicomponent liquid systems has been a topic of increasing interest in recent years. The incentives for research in this field have evolved from both practical and theoretical considerations. Many common chemical engineering processes such as catalysis and adsorption depend upon mass transfer by means of molecular diffusion. Molecular diffusion also plays a vital role in a wide variety of biological processes. In many cases the design of a commercial process or the understanding of a natural process requires the knowledge of multicomponent diffusion coefficients. Thus it may be seen that research in diffusion has a real practical value.

Because of the complexity and difficulty of experimentally studying multicomponent diffusion, there has been relatively little data reported. Faced with this scarcity of data, the engineer is often forced to turn to predictive techniques or approximations. These techniques, in turn,

depend upon experimental data for their development. To this date multicomponent diffusion data has been presented for ternary systems only. It is questionable, therefore, whether predictive techniques based upon this data may safely be extended to systems of higher order.

Although theoretical knowledge of the gaseous and solid states is quite advanced, an adequate model for the complicated liquid state does not yet exist. Experimental study of diffusion in liquids provides data which may be used as an excellent test of proposed theories. Thus, research in multicomponent diffusion also is of interest from a theoretical viewpoint.

The history of the study of molecular diffusion begins with Fick (27), who proposed that the diffusion process was analogous to heat conduction in solids. Since Fick presented his equation which defines the diffusion coefficient, there has been extensive experimental and theoretical research in the field of molecular diffusion. Most of the work has been concentrated on study of self and infinite dilution diffusion or on diffusion in binary systems. The first experimental study of diffusion in a ternary system was carried out in 1955 by Baldwin, Dunlop, Fujita and Gosting (3, 28). Since that time refinements in experimental techniques have improved the accuracy of measured diffusivities and decreased the complications in obtaining them. Multicomponent diffusivities have been

measured for about twenty-eight ternary systems. Most of the reported measurements, however, cover only a limited concentration or temperature range.

The most general description of the diffusion process in a multicomponent solution is provided by the theory of irreversible thermodynamics, which was first presented by Onsager (41, 42). Through consideration of an entropy balance the following relation describing the flux of each component in a multicomponent solution may be developed,

$$J_i = \sum_{j=1}^{N-1} L_{ij} Y_j \quad i=1, \dots, N-1 \quad (1)$$

where J_i is the flux of component i , Y_j is the thermodynamic driving force which is related to the gradient of chemical potential, the terms L_{ij} are the phenomenological coefficients, and N is the number of components in the system. Details of the derivation of Equation (1) are given by DeGroot and Mazur (14). An important result of irreversible thermodynamics states that the matrix of phenomenological coefficients is symmetric, that is

$$L_{ij} = L_{ji} \quad i, j=1, \dots, N-1 \quad (2)$$

These relations, which have become known as the Onsager reciprocal relations, are important because they reduce the number of parameters necessary to describe multicomponent diffusion.

Unfortunately, it is not possible to measure the thermodynamic forces Y_j in the course of a diffusion experiment. Baldwin, Dunlop and Gosting (3), however, have presented equations relating the fluxes to gradients of concentration.

$$J_i = - \sum_{j=1}^{N-1} D_{ij} \frac{\partial C_j}{\partial X} \quad i=1, \dots, N-1 \quad (3)$$

where C_j is the concentration of component j , X is the physical length in the direction of diffusion, and D_{ij} is the multicomponent diffusion coefficient relating the flux of component i to the gradient of component j . The magnitudes of the diffusivities in Equation (3) depend upon the units of concentration and flux, and upon the frame of reference for the fluxes. Equation (3) provides the basis for experimental study of the diffusion process in multicomponent solutions.

In this research a technique was developed for the experimental determination of diffusion coefficients in a four component system. This technique will be valuable in that it will allow tests of predictive techniques for systems of more than three components, and it will allow further tests of the Onsager reciprocal relations. This experimental technique was used to study one quaternary system over a moderate concentration range at 25°C.

A separate part of this research was the development of a predictive technique for multicomponent diffusion

based upon the Enskog theory of diffusion in a rigid sphere fluid and a continuous association model. This technique allows prediction of multicomponent diffusivities without the necessity of having thermodynamic data.

CHAPTER II

EXPERIMENTAL INVESTIGATIONS

Background

The experimental measurement of molecular diffusion coefficients in liquids has been accomplished through a wide variety of methods. The techniques used include steady-state methods, restricted diffusion methods, methods based on diffusion in laminar streams, and methods based on a free diffusion model.

The usual steady-state diffusion process includes two relatively large reservoirs of different concentrations separated by a porous diaphragm. Diffusion occurs across the diaphragm, and the concentrations in the reservoirs are monitored continuously or at regular intervals. Using various modifications of the diaphragm cell technique, the following ternary systems have been studied: acetone-benzene-carbon tetrachloride (9); mannitol-NaCl-water, pentaerythritol-NaCl-water (36); methanol-n-propanol-isobutanol (46); sucrose-KCl-water, sucrose-glucose-water, sucrose-fructose-water (4); benzene-2-propanol-carbon tetrachloride (30); n-hexane-n-tetradecane-toluene, n-hexane-cyclohexane-toluene,

cyclohexane-n-decane-toluene (34); sucrose-glucose-water, sucrose-raffinose-water, and glucose-raffinose-water (29). The diaphragm cell's advantages include simplicity and ease of analysis of the data. The principal disadvantage of this method is that calibration with a substance for which the diffusivity is known is required.

In general, it has been found that free diffusion methods provide the most accurate and consistent values for diffusion coefficients. In a free diffusion experiment, a horizontal boundary is formed between two solutions of slightly different concentration, the more dense solution being on the bottom. As mutual diffusion occurs the concentration on each side of the initial interface changes. This process may be described as free diffusion as long as the concentrations at the ends of the cell remain constant. The diffusion coefficients which determine the rate of molecular flux may be determined by measuring the concentrations as a function of time and the distance from the initial boundary. The concentrations are usually determined by relating them to the refractive index of the solution. This technique requires that the solutions be transparent and that the relation between the refractive index and the concentration be known.

The most widely used free diffusion method is the Gouy interference method. This technique consists of passing a converging light beam through the diffusion cell

containing the diffusing solutions. The concentration gradient in the cell causes the formation of a series of fringes which may be recorded and used to determine the diffusion coefficients. The following ternary systems have been studied with experimental techniques based on the free diffusion model: LiCl-NaCl-water, LiCl-KCl-water (19); NaCl-KCl-water (17,20); Na_2SO_4 - H_2SO_4 -water (53); KCl-glycine-water (55); KCl-raffinose-water (15); KCl-sucrose-water (45); NaCl-mannitol-water (18); NaCl-pentaerythritol-water (54); glucose-sucrose-water (52); sucrose-glycine-water (21); sucrose-mannitol-water (26); raffinose-urea-water (16); urea-urea(+)-water (1); polystyrene-cyclohexane-toluene (12); toluene-chlorobenzene-bromobenzene (6); polystyrene 1-polystyrene 2-toluene (13); dodecane-hexadecane-decane, diethyl ether-chloroform-carbon tetrachloride (37); acetone-benzene-methanol, acetone-ethanol-water (2).

Experimental Apparatus

In this research an optical method based on the free diffusion model was used. The experimental apparatus was developed and constructed by Merliss (40) and was modified by Haluska (32) and Alimadadian (2). The apparatus employs a double Savart plate birefringent interferometer to measure the refractive index profile within the diffusion cell. Bryngdahl (5) has shown that this instrument is capable of detecting very small differences in refractive index.

Thus only small concentration differences between the two solutions are required. This capability is a great advantage because it insures that the refractive index will be a linear function of concentration, the diffusion coefficients will be nearly constant throughout the diffusion region, and the effects of volume changes as a result of mixing will be minimal.

In order to perform a free diffusion experiment, a step function in concentration at the interface between the two solutions must be formed. Although it is impossible to form a perfect interface between the two solutions, a close approximation to this condition was accomplished through use of a flowing junction test cell. This cell, which is shown schematically in Figure 1, was designed by Alimadadian (2) and was similar to the cell used by Svenson (49) and Skinner (47). The cell was constructed of stainless steel and was jacketed with copper plates. The diffusion cavity was $3\frac{1}{2}$ inches high, $\frac{1}{4}$ inch wide, and three inches deep. A slit 0.006 inches wide was cut on either side of the cavity at the centerline for the withdrawal of fluid during interface formation. The ends of the cell were covered with two windows of high quality optical glass. Openings were provided at the top and bottom of the cell for filling, draining, and venting.

Because the diffusion process is very sensitive to temperature, the entire diffusion cell and the stainless

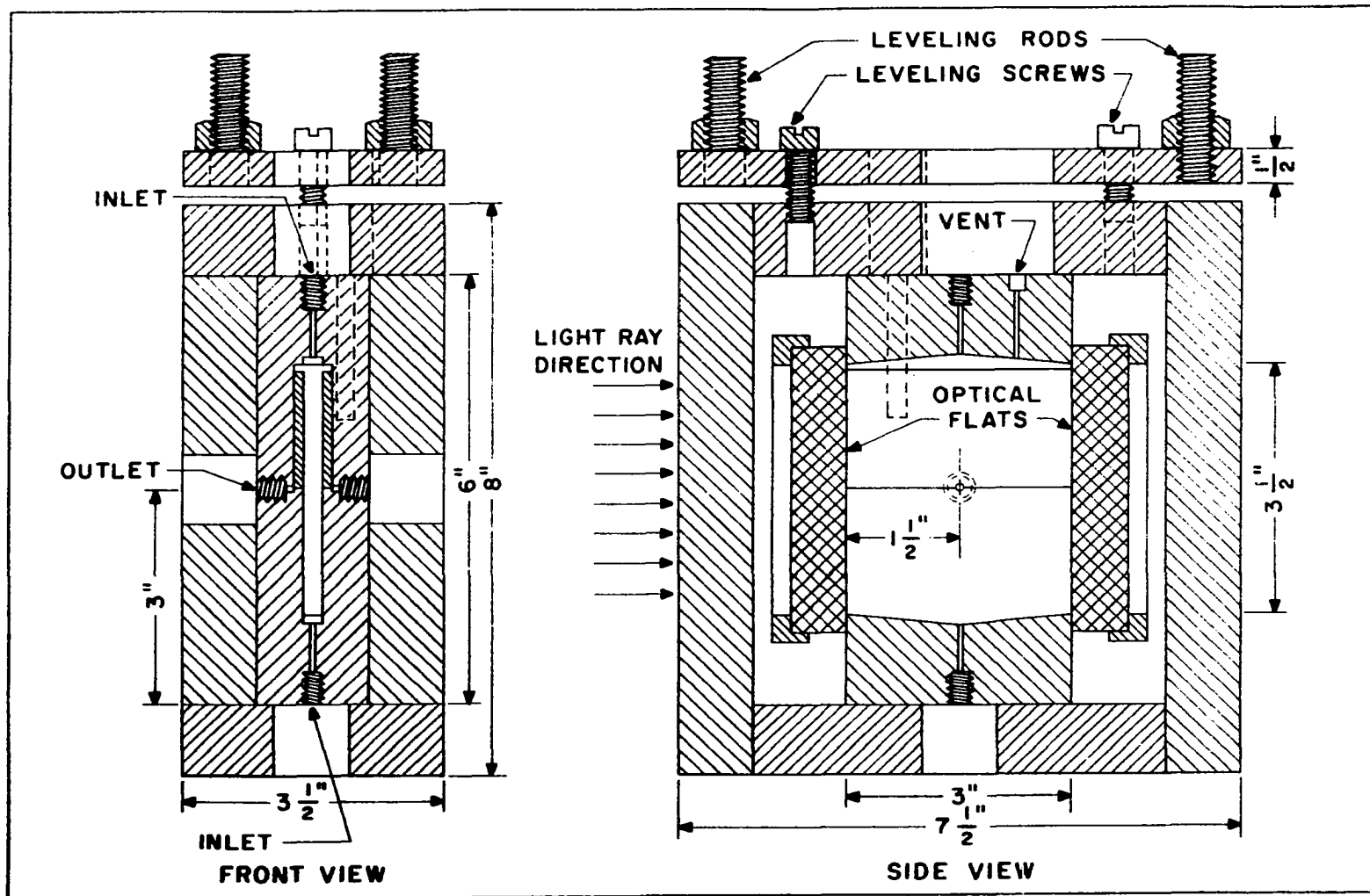
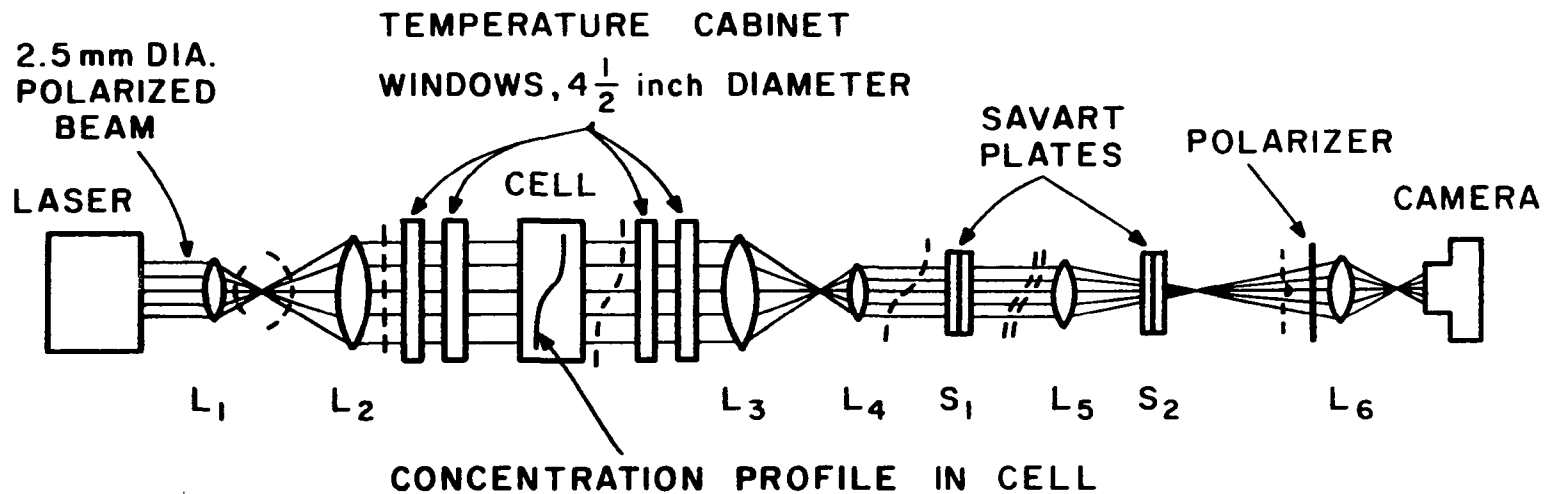


Figure 1. Flowing Junction Test Cell

steel fluid reservoirs were contained inside a constant temperature air bath. The air bath consisted of a double wall insulated box, heater elements, cooling coils, baffles, a fan, and a platinum resistance thermometer. Windows were installed in each side of the air bath for observation and for passage of the interferometer beam through the diffusion cell. A Hallikainen Thermotrol was used to control the temperature within the air bath to 0.01°C . The temperature in the system was determined by measuring the resistance of the platinum resistance thermometer with a Mueller Temperature Bridge and referring to appropriate calibration charts.

The birefringent interferometer used is illustrated in Figure 2. The light source for the interferometer is provided by a helium-neon gas laser. The spatially and temporally coherent beam from the laser is magnified by lenses L_1 and L_2 and passes through the diffusion cell. If a refractive index gradient exists in the liquid in the cell, the wavefront is modified as it passes through. Lenses L_3 and L_4 demagnify the beam, and it then passes through Savart plate S_1 . This Savart plate splits the beam into two parallel, slightly displaced parts. After passing through lens L_5 , the beam enters Savart plate S_2 which causes a small angle to be formed between the two displaced wavefronts. This small angle causes the formation of interference patterns which may be viewed after the beam passes



- | | |
|---|--|
| L ₁ - 18.3 mm DIA. , 39 mm f/l | L ₅ - 35 mm DIA. , 63 mm f/l |
| L ₂ , L ₃ - 4 1/8 inch DIA. , 60 inch f/l | L ₆ - 36 mm DIA. , 100 mm f/l |
| L ₄ - 35 mm DIA. , 200 mm f/l | |

NOTE :

DASHED LINES REPRESENT SHAPE OF LIGHT FRONT AT POINT INDICATED

Figure 2. Interferometer Optical Arrangement

through a polarizer. All components of the interferometer were mounted on a heavy optical bench in order to reduce vibration.

The interference patterns which indicated the refractive index gradients in the fluid in the diffusion cell were recorded on film with a Nikkormat FT 35mm camera. The film used was Kodak Plus-X Panchromatic.

The apparatus just described has been successfully used in four previous investigations (40, 32, 2, 51). In these studies the validity of this experimental method has been repeatedly confirmed for both binary and ternary diffusion.

Experimental Technique

Before a diffusion experiment may be carried out, several preliminary operations must be performed. First, the alignment of the apparatus including the laser, lenses, diffusion cell and air bath windows must be checked. The details of this procedure are described by Merliss (40).

Next the cell, reservoirs, and the accompanying tubings must be thoroughly cleaned to remove any trace of chemicals from a previous run. The cleaning operation was accomplished by rinsing the apparatus several items with acetone and drying with compressed air. The system was also carefully checked for leaks during the cleaning operation.

The preparation of solutions is a critical step in the experimental procedure, especially for a run with a multicomponent system. An N-component system requires at least N-1 runs, each at the same average concentration. Also, the concentration difference for each run must be adjusted for a proper difference in refractive index. A refractive index difference of about 1.0×10^{-4} was found to give good results at most concentrations.

The solutions were prepared by first mixing a large enough quantity of solution for all runs at the desired average concentration. The mixture was then divided into smaller portions for use in each of the runs. Approximately 150 ml. each of high density and low density solution were required for each run.

In order to provide a concentration difference between the top and bottom solutions, small quantities of the pure components were added to each portion of the base solution. For quaternary systems, usually three pure components were added to each portion. The amount of each pure component to be added was calculated to provide the proper difference in refractive indexes and to insure that the diffusion path would be different for each run. This calculation was facilitated by a computer program written for the PDP-8 computer. Each incremental quantity of the pure components was carefully weighed in a small weighing bottle and was then added to the appropriate solution.

After filling the fluid reservoirs with the proper solutions, the lid of the temperature bath was replaced, and procedures were initiated for bringing the bath temperature to the desired level. The set point on the Thermotrol was adjusted to maintain the proper temperature as observed by using the platinum resistance thermometer in conjunction with the Mueller Temperature Bridge. The system was allowed to equilibrate for at least two hours after reaching running temperature to insure that there were no temperature gradients in the solutions or in the diffusion cell.

Formation of the diffusion interface was begun by filling the cell with the heavy solution through the opening in the bottom of the cavity. Then the lighter solution was allowed to flow into the cell by closing the valve to the heavy reservoir, closing the vent, opening the valve to the light reservoir, and slowly opening the valve controlling flow out of the slits in the sides of the cell. The interface thus formed between the two solutions slowly moved from the top of the cell to the middle. At this point flow was again started from the bottom of the cell. The interface was sharpened by observing it through the camera viewfinder and adjusting the drip rate and the flows from the two reservoirs.

After the interface had reached its maximum sharpness and after all disturbances in the fluid column were gone, the run was started. Simultaneously, the flows from

the two reservoirs and out of the slits were interrupted, and the electric timer was started. The progress of the diffusion was followed visually, and pictures were taken throughout the run. Usually about 15 exposures were made during each run.

Materials

The chemicals used in this study were all pure grade chemicals donated by Phillips Petroleum Company. The specifications for these chemicals as given by Phillips are detailed in Appendix B. The chemicals were used as received without further purification.

Data Analysis

Molecular diffusion in a one dimensional multicomponent system of N components may be described by an extension of Fick's second law as follows:

$$\frac{\partial C}{\partial t} = -D \frac{\partial^2 C}{\partial X^2} \quad (4)$$

where C is the vector of solute concentrations of order N-1, and D is the N-1xN-1 matrix of diffusion coefficients. Thus for a quaternary system, it is necessary to determine nine parameters from the experimental data. The appropriate initial and boundary conditions for Eq. (4) are:

$$\begin{aligned}
C &= \bar{C} + \frac{\Delta C}{2} \text{ for } X > 0, t = 0 \\
C &= \bar{C} - \frac{\Delta C}{2} \text{ for } X < 0, t = 0 \\
C &\rightarrow \bar{C} + \frac{\Delta C}{2} \text{ for } X \rightarrow \infty, t > 0 \\
C &\rightarrow \bar{C} - \frac{\Delta C}{2} \text{ for } X \rightarrow -\infty, t > 0
\end{aligned} \tag{5}$$

where \bar{C} is the vector of mean concentrations and ΔC is the vector of concentration differences.

The solution to Eq. (4) with the conditions given by Eq. (5) is detailed in Appendix A. The result for each component is given by the following equations,

$$\hat{C}_i = \frac{1}{2}(\hat{C}_i(\infty) - \hat{C}_i(-\infty)) + \frac{1}{2}(\hat{C}_i(-\infty) - \hat{C}_i(\infty)) \operatorname{erf}(\eta_i) \tag{6}$$

$$C = M\hat{C} \tag{7}$$

$$\eta_i = \frac{X}{2\sqrt{\lambda_i t}} \tag{8}$$

where λ_i is the i th eigenvalue of the matrix D , and M is the modal matrix of D (i.e., the column vectors of M are eigenvectors of D). If Eq. (7) is solved for C_i and the result substituted in Eq. (6), the following is obtained,

$$(C - \bar{C})_i = \frac{1}{2} \sum_{j=1}^{N-1} \left(\sum_{k=1}^{N-1} (M_{jk}^{-1} \Delta C_k) M_{ij} \operatorname{erf}(\eta_j) \right) \tag{9}$$

where M_{jk}^{-1} is an element of the inverse of matrix M . Thus the solute concentrations are determined by the modal matrix of the diffusivity matrix and its eigenvalues. If the value of each M_{ij} and each λ_i may be determined from the experimental

results, then the diffusion coefficients may be found through the following expression,

$$D = MSM^{-1} \quad (10)$$

where S is the diagonal matrix with elements $\lambda_1, \dots, \lambda_{N-1}$ in the principal diagonal.

The concentration gradients in the diffusion cell may be related to the interference patterns recorded on the film by assuming that the refractive index, n , of the solution is a linear function of the solute concentrations. This relationship may be expressed as

$$n = \bar{n} + \sum_{i=1}^{N-1} R_i (C - \bar{C})_i \quad (11)$$

where \bar{n} is the refractive index of the solution having the average concentrations, and R_i is given by

$$R_i = \left[\frac{\partial n}{\partial C_i} \right] \quad (12)$$

The optical path length is defined as the product of the refractive index and the length of the diffusion cell, α . Combining this definition with Eq. (11) gives

$$Z = \alpha n = \alpha \left(\bar{n} + \sum_{i=1}^{N-1} R_i (C - \bar{C})_i \right)$$

The images recorded on the film represent the derivative of the optical path length with respect to vertical distance in the cell, thus

$$\left(\frac{\partial Z}{\partial X} \right)_t = \alpha \sum_{i=1}^{N-1} R_i \left(\frac{\partial C_i}{\partial X} \right)_t \quad (14)$$

The partial derivative of C_i with respect to X may be found from Eq. (9),

$$\left(\frac{\partial C_i}{\partial X}\right)_t = \frac{1}{2} \sum_{j=1}^{N-1} \left(\sum_{K=1}^{N-1} (M_{jK}^{-1} \Delta C_K) \frac{M_{ij}}{\sqrt{\pi t \lambda_j}} \exp\left(\frac{-X^2}{4\lambda_j t}\right) \right) \quad (15)$$

Substituting Eq. (15) in Eq. (14) yields

$$\left(\frac{\partial Z}{\partial X}\right)_t = \frac{\alpha}{2\sqrt{\pi t}} \sum_{i=1}^{N-1} R_i \sum_{j=1}^{N-1} (M_{jk}^{-1} \Delta C_K) \frac{M_{ij}}{\sqrt{\lambda_j}} \exp\left(\frac{-X^2}{4\lambda_j t}\right) \quad (16)$$

Rearranging Eq. (16) gives

$$\left(\frac{\partial Z}{\partial X}\right)_t = \frac{\alpha}{2\sqrt{\pi t}} \sum_{i=1}^{N-1} \left(\sum_{K=1}^{N-1} (M_{iK}^{-1} \Delta C_K) \frac{1}{\sqrt{\lambda_i}} \sum_{j=1}^{N-1} (R_j M_{ji}) \exp\left(\frac{-X^2}{4\lambda_i t}\right) \right) \quad (17)$$

Let a new variable P_i be defined as follows,

$$P_i = \sum_{K=1}^{N-1} (M_{iK}^{-1} \Delta C_K) \sum_{j=1}^{N-1} (R_j M_{ji}) \quad (18)$$

Substituting P_i in Equation (17) yields

$$\left(\frac{\partial Z}{\partial X}\right)_t = \frac{\alpha}{2\sqrt{\pi t}} \sum_{i=1}^{N-1} \frac{P_i}{\sqrt{\lambda_i}} \exp\left(\frac{-X^2}{4\lambda_i t}\right) \quad (19)$$

From Eq. (18) it may be shown that the following relation between the P_i 's holds

$$\sum_{i=1}^{N-1} P_i = \Delta n \quad (20)$$

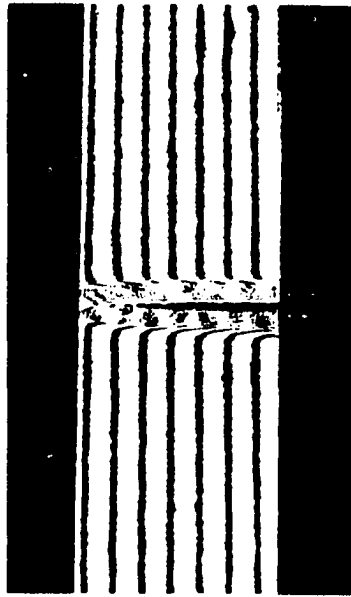
where Δn is the total difference in refractive index between the top and bottom solutions. Equation (19) is the final

result which was used to interpret the photographs of the interference patterns. It may be noted that the maximum value of $\left(\frac{\partial Z}{\partial X}\right)_t$ may be found by setting $X=0$ in Eq. (19).

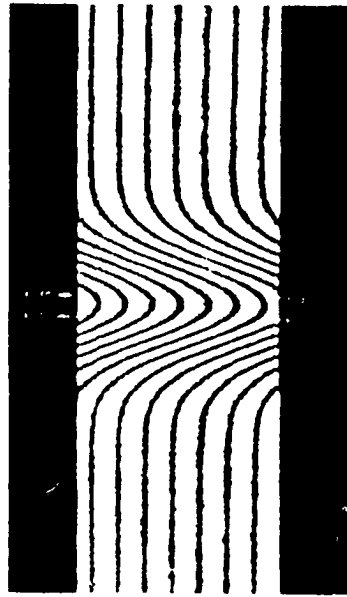
The data analysis procedure may be summarized at this point as follows. First the parameters P_i and λ_i are formed which allow the model represented by Eq. (19) to most accurately reproduce the experimental data. Next, Eq. (18) is used with the results from $N-1$ runs to calculate the elements of the modal matrix M . Finally, Eq. (10) is used to calculate the $(N-1)^2$ diffusion coefficients. These steps will be explained in more detail in the following paragraphs.

Figure 3 illustrates the appearance of the interference patterns produced in a typical experiment. One of the fringes was selected for measurement throughout each set of photographs. The necessary data from each curve included the maximum height of the curve, h ; the height, h , and the width, w , of the curve at several points; the area under the curve; and the first and second semi-moments of the curve. The width of the cell was also measured in order to provide a reference for scaling the other dimensions.

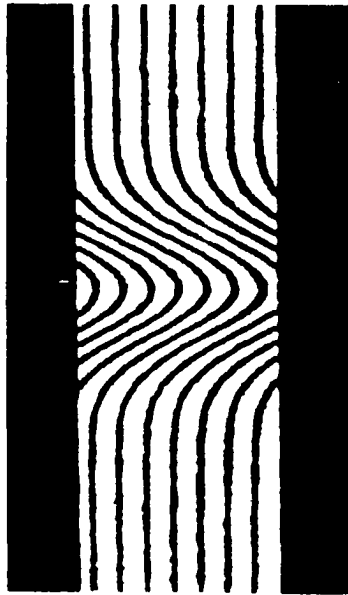
The measurement of the developed negatives was accomplished with a microprojector equipped with a movable stage controlled by tubular micrometers. This apparatus allowed measurements to within 0.0005 inches. An interdata computer equipped with a pencil-follower was used to



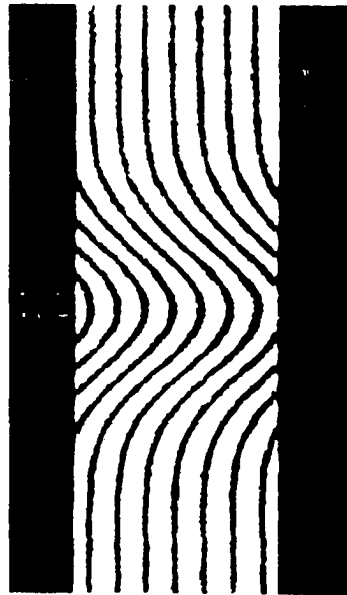
Initial Interface



t = 1200 sec



t = 1715 sec



t = 3000 sec

Figure 3. Photographs of Initial Interface and Interference Patterns

determine the areas and moments of the curve. The pencil-follower apparatus consisted of a flat table, a lens with crosshairs which could be moved over the surface of the table, and a device under the table which determined the position of the crosshairs to within 0.1mm. The coordinates of the point determined by the crosshairs were continually transmitted to the computer where they could be used as desired in a program. Thus by slowly moving the crosshairs along the fringe pattern and by using the proper computer program, it was possible to determine the areas and moments of the optical path gradient curve with speed and accuracy.

After extracting the required data from the photographs of the fringe patterns, the parameters P_i and λ_i in Eq. (19) were determined. Equation (19) represents a valid model for diffusion in a system in which there is an infinitely sharp interface at the start of the experiment. As noted previously, it is impossible to form a perfect interface. Therefore, it is necessary to modify the experimental data to account for this imperfection. It may be shown that, except for a time difference, the concentration profiles which result from an imperfect interface approach those resulting from an ideal interface after irregularities die out. An equation relating each experimental time, t_j , and the maximum height of the concentration gradient curve, $h \max_j$, may be found from Eq. (19),

$$t_j = a \left(\frac{1}{h \max_j} \right)^2 - t_0 \quad (21)$$

where a is a constant and t_0 is the zero time correction. A least squares analysis based on Eq. (21) and the experimental values of t_j and $h \max_j$ was used to determine the zero time correction. In subsequent paragraphs it will be assumed that the times t_j have been adjusted by addition of t_0 .

In order to find the best values for the $N-1$ P_i 's and λ_i 's in Eq. (20), it was found that two separate methods of solution were required. A direct least squares fit of Eq. (20) to the experimental values of h_j , t_j , and w_j yielded the most accurate values for the parameters P_i and λ_i . However, no method was found for the determination of these parameters which did not require fairly good initial guesses. Therefore another method was used which was based on the areas and moments of the diffusion gradient curve. This method did not provide the accuracy of the direct approach, but it was found to be a stable method which gave sufficiently close values for subsequent use in the first method. The details of the area-moment method will be given first.

The area under the concentration gradient curve may be found from Eq. (19).

$$A = 2 \int_0^{\infty} \left(\frac{\partial Z}{\partial X} \right)_t dx = \alpha \sum_{i=1}^{N-1} P_i = \alpha \Delta n \quad (22)$$

Thus, the area under the concentration gradient curve is constant throughout the run. The maximum height of the curve is at $X=0$ and may also be found from Eq. (19),

$$\left(\frac{\partial Z}{\partial X}\right)_{t_{\max}} = \frac{\alpha}{2\sqrt{\pi t}} \sum_{i=1}^{N-1} \frac{P_i}{\sqrt{\lambda_i}} \quad (23)$$

The reduced height to area ratio is defined as

$$DA = \frac{2\sqrt{\pi t} \Delta n \left(\frac{\partial Z}{\partial X}\right)_{t_{\max}}}{A} = \sum_{i=1}^{N-1} \frac{P_i}{\sqrt{\lambda_i}} \quad (24)$$

For a quaternary system it is also necessary to measure the first and second semi-moments of the curve. The first semi-moment of the concentration gradient curve is defined as

$$M = 2 \int_0^{\infty} X \left(\frac{\partial Z}{\partial X}\right)_t dX = 2\alpha\sqrt{\frac{t}{\pi}} \sum_{i=1}^{N-1} P_i \sqrt{\lambda_i} \quad (25)$$

The reduced first moment is given by

$$DM = \frac{\Delta n}{2} \sqrt{\frac{\pi}{t}} \frac{M}{A} = \sum_{i=1}^{N-1} P_i \sqrt{\lambda_i} \quad (26)$$

The second semi-moment is found in a similar manner

$$S = 2 \int_0^{\infty} X^2 \left(\frac{\partial Z}{\partial X}\right)_t dX = 2\alpha t \sum_{i=1}^{N-1} P_i \lambda_i \quad (27)$$

Finally, the reduced second moment is defined as

$$DS = \frac{S}{2} \frac{\Delta n}{At} = \sum_{i=1}^{N-1} P_i \lambda_i \quad (28)$$

Equations (20), (24), (26) and (28) provide four independent relationships between the six variables which must be determined for a quaternary system (i.e., P_i , λ_i , $i=1, 2, 3$). Since there are insufficient equations to solve for the parameters, it is necessary to make duplicate experimental runs with the same average concentrations, but with different concentration differences. For such runs the parameter λ_i will remain constant, but the P_i 's will vary. Thus for three runs at the same average concentration there will be nine different P_i 's and three λ_i 's, and the four equations above will provide the necessary relationships for their determination. The twelve resulting equations may be written as follows:

$$DA^1 = \frac{P_1^1}{\sqrt{\lambda_1}} + \frac{P_2^1}{\sqrt{\lambda_1}} + \frac{P_3^1}{\sqrt{\lambda_1}} \quad (29-1)$$

$$DA^2 = \frac{P_1^2}{\sqrt{\lambda_1}} + \frac{P_2^2}{\sqrt{\lambda_2}} + \frac{P_3^2}{\sqrt{\lambda_3}} \quad (29-2)$$

$$DA^3 = \frac{P_1^3}{\sqrt{\lambda_1}} + \frac{P_2^3}{\sqrt{\lambda_2}} + \frac{P_3^3}{\sqrt{\lambda_3}} \quad (29-3)$$

$$DM^1 = P_1^1 \sqrt{\lambda_1} + P_2^1 \sqrt{\lambda_2} + P_3^1 \sqrt{\lambda_3} \quad (29-4)$$

$$DM^2 = P_1^2 \sqrt{\lambda_1} + P_2^2 \sqrt{\lambda_2} + P_3^2 \sqrt{\lambda_3} \quad (29-5)$$

$$DM^3 = P_1^3 \sqrt{\lambda_1} + P_2^3 \sqrt{\lambda_2} + P_3^3 \sqrt{\lambda_3} \quad (29-6)$$

$$DS^1 = P_1^1 \lambda_1 + P_2^1 \lambda_2 + P_3^1 \lambda_3 \quad (29-7)$$

$$DS^2 = P_1^2 \lambda_1 + P_2^2 \lambda_2 + P_3^2 \lambda_3 \quad (29-8)$$

$$DS^3 = P_1^3 \lambda_1 + P_2^3 \lambda_2 + P_3^3 \lambda_3 \quad (29-9)$$

$$\Delta n^1 = P_1^1 + P_2^1 + P_3^1 \quad (29-10)$$

$$\Delta n^2 = P_1^2 + P_2^2 + P_3^2 \quad (29-11)$$

$$\Delta n^3 = P_1^3 + P_2^3 + P_3^3 \quad (29-12)$$

where the superscripts refer to each of the three different runs. The system of equations above is non-linear, and no straightforward method of solution is available. Therefore, the parameters were determined by converting the equations to a minimization problem. A variable Q to be minimized is defined as follows:

$$Q = \sum_{i=1}^3 (DS^i - \sum_{j=1}^3 P_j^i \lambda_j)^2 \quad (30)$$

Thus it was necessary to find the values of the variables P^i and λ_j which produced the minimum Q and which also satisfied the other equations. The minimization problem was solved by using a direct search technique called pattern search which was first developed by Hooke and Jeeves (35). Details of this method are given in Appendix (D).

The values of the parameters P_i^j and λ_i found by the procedure outlined above were used in a subsequent step to refine their values. The ratio of the height of the concentration gradient curve at any point to the maximum height at $X=0$ may be found from Eqs. (19) and (23),

$$\bar{Z} = \frac{1}{\sum_{i=1}^{N-1} \frac{P_i}{\sqrt{\lambda_i}}} \sum_{i=1}^{N-1} \frac{P_i}{\sqrt{\lambda_i}} \exp\left(\frac{-X^2}{4\lambda_i t}\right) \quad (31)$$

The experimental values of \bar{Z} , X , and t from several points on three different runs were used to determine the values of the parameters which gave the least total deviation from the model represented by Eq. (31). The pattern search algorithm was again used to determine the parameters.

The next step in the data analysis is the calculation of the modal matrix of the diffusivity matrix. Since the column vectors of M are eigenvectors of D , one element in each column is arbitrary. Correspondingly, each row of the inverse of M contains one arbitrary element. Letting each element of the first column of the matrix M^{-1} be equal to unity, the following system of equations may be developed from Eq. (18),

$$P_1^1 = (\Delta C_1^1 + M_{12}^{-1} \Delta C_2^1 + M_{13}^{-1} \Delta C_3^1) (R_1 M_{11} + R_2 M_{21} + R_3 M_{31}) \quad (32)$$

$$P_2^1 = (\Delta C_1^1 + M_{22}^{-1} \Delta C_2^1 + M_{23}^{-1} \Delta C_3^1) (R_1 M_{12} + R_2 M_{22} + R_3 M_{32}) \quad (33)$$

$$P_1^2 = (\Delta C_1^2 + M_{12}^{-1} \Delta C_2^2 + M_{13}^{-1} \Delta C_3^2) (R_1 M_{11} + R_2 M_{21} + R_3 M_{31}) \quad (34)$$

$$P_2^2 = (\Delta C_1^2 + M_{22}^{-1} \Delta C_2^2 + M_{23}^{-1} \Delta C_3^2) (R_1 M_{12} + R_2 M_{22} + R_3 M_{32}) \quad (35)$$

$$P_1^3 = (\Delta C_1^3 + M_{12}^{-1} \Delta C_2^3 + M_{13}^{-1} \Delta C_3^3) (R_1 M_{11} + R_2 M_{21} + R_3 M_{31}) \quad (36)$$

$$P_2^3 = (\Delta C_1^3 + M_{22}^{-1} \Delta C_2^3 + M_{23}^{-1} \Delta C_3^3) (R_1 M_{12} + R_2 M_{22} + R_3 M_{32}) \quad (37)$$

where M_{ij}^{-1} is an element of M^{-1} and M_{ij} is an element of M .

Let the variables T_1 and T_2 be defined as follows:

$$T_i = R_1 M_{1i} + R_2 M_{2i} + R_3 M_{3i} \quad (38)$$

Substituting T_1 into Eqs. (32), (34) and (36) gives

$$P_1^1 = \Delta C_1^1 T_1 + \Delta C_2^1 (T_1 M_{12}^{-1}) + \Delta C_3^1 (T_1 M_{13}^{-1}) \quad (39)$$

$$P_2^2 = \Delta C_1^2 T_1 + \Delta C_2^2 (T_1 M_{12}^{-1}) + \Delta C_3^2 (T_1 M_{13}^{-1}) \quad (40)$$

$$P_3^3 = \Delta C_1^3 T_1 + \Delta C_2^3 (T_1 M_{12}^{-1}) + \Delta C_3^3 (T_1 M_{13}^{-1}) \quad (41)$$

By considering the products $T_1 M_{12}^{-1}$ and $T_1 M_{13}^{-1}$ as single variables, Eqs. (39), (40) and (41) may be solved for T_1 , M_{12}^{-1} and M_{13}^{-1} .

Using Eqs. (33), (35) and (37) in a similar manner, the values of T_2 , M_{22}^{-1} and M_{23}^{-1} may be determined.

The elements M_{32}^{-1} and M_{33}^{-1} remain to be determined. If Eq. (38) is expanded in terms of the inverse elements, the result upon rearrangement is

$$\begin{aligned} T_1 [M_{13}^{-1}M_{22}^{-1} - M_{12}^{-1}M_{23}^{-1}] + R_2M_{23}^{-1} - R_3M_{22}^{-1} &= [T_1 (M_{13}^{-1} - M_{23}^{-1}) \\ &+ R_1M_{23}^{-1} - R_3]M_{32}^{-1} + [T_1 (M_{22}^{-1} - M_{12}^{-1}) - R_1M_{22}^{-1} + R_2]M_{33}^{-1} \end{aligned} \quad (42)$$

$$\begin{aligned} T_2 [M_{13}^{-1}M_{22}^{-1} - M_{12}^{-1}M_{23}^{-1}] - R_2M_{13}^{-1} + R_3M_{12}^{-1} &= [T_2 (M_{13}^{-1} - M_{23}^{-1}) \\ &- R_1M_{13}^{-1} + R_3]M_{32}^{-1} + [T_2 (M_{22}^{-1} - M_{12}^{-1}) + R_1M_{12}^{-1} - R_2]M_{33}^{-1} \end{aligned} \quad (43)$$

The only unknowns in Eqs. (42) and (43) are M_{32}^{-1} and M_{33}^{-1} . After solving for M_{32}^{-1} and M_{33}^{-1} , the modal matrix may be found by inversion of M^{-1} .

The final step in the data analysis is calculation of the elements of D. Since each element of M and M^{-1} has been determined, as well as the eigenvalues λ_i , Eq. (10) may be used to calculate D.

In order to provide additional information concerning the quarternary system studied, infinite dilution binary runs were made with each combination of components. The experimental techniques used for binary diffusion are similar to those used for a multicomponent system. The

analysis of the experimental data, however, is considerably less complicated. A new method of analysis was developed for binary diffusion which does not require iterative calculations. Details of this technique are outlined in Appendix C.

Experimental Results

The system selected for experimental study in this work was a four component system consisting of toluene, cyclohexane, n-heptane, and n-decane. The basis for selection of this system was primarily an adequate range in the refractive indices and densities of the pure components.

As mentioned previously, analysis of the results of a quaternary diffusion experiment requires three runs at each concentration studied. By making four runs at each concentration, it was possible to determine an approximate error in the results. The four runs were combined three ways to provide multiple results.

The results for the diffusion matrix at each concentration studied are given in Table 1. In the calculation of these results the component n-decane was arbitrarily selected as the solvent. The diffusion coefficients given represent an average of the three calculations as mentioned above. The limits given are the maximum observed deviations from the average.

TABLE I

MOLECULAR DIFFUSION COEFFICIENTS AT 25°C FOR
 THE SYSTEM CYCLOHEXANE(1) - TOLUENE(2) -
 n-HEPTANE(3) - n-DECANE(4)

Weight Fractions			Diffusion Matrix		
W_1	W_2	W_3	$D \times 10^5, \text{cm}^2/\text{Sec}$		
.25	.25	.25	1.94±0.05	-0.07±0.08	-0.14±0.04
			0.02±0.09	1.98±0.06	-0.17±0.03
			-0.18±0.06	-0.07±0.05	1.73±0.09
.20	.30	.40	2.11±0.12	0.03±0.09	-0.10±0.07
			-0.16±0.05	1.99±0.08	-0.19±0.10
			-0.22±0.06	-0.14±0.07	1.86±0.11
.30	.30	.30	1.84±0.08	-0.16±0.03	0.08±0.11
			-0.12±0.07	1.79±0.12	0.01±0.05
			-0.08±0.06	-0.11±0.04	1.65±0.06
.15	.15	.60	2.44±0.14	-0.09±0.08	0.03±0.07
			-0.05±0.06	2.70±0.10	-0.02±0.07
			-0.28±0.09	-0.35±0.16	1.92±0.06
.15	.60	.15	2.01±0.09	-0.06±0.03	-0.02±0.05
			-0.33±0.07	1.83±0.04	-0.22±0.10
			0.04±0.06	-0.03±0.02	1.93±0.11
.60	.15	.15	1.55±0.16	-0.28±0.08	-0.16±0.06
			0.04±0.09	1.71±0.09	-0.03±0.05
			0.05±0.02	-0.12±0.05	1.62±0.11
.44	.44	.02	1.59±0.07	-0.33±0.14	-0.21±0.06
			-0.36±0.08	1.77±0.11	-0.29±0.04
			0.08±0.05	0.01±0.12	1.49±0.09
.44	.02	.44	2.06±0.04	-0.21±0.08	-0.31±0.10
			0.10±0.13	2.27±0.09	-0.01±0.05
			-0.33±0.06	-0.41±0.11	1.76±0.14
.02	.44	.44	3.01±0.22	0.06±0.11	0.02±0.06
			-0.44±0.13	2.30±0.09	0.38±0.09
			-0.52±0.09	-0.25±0.06	2.33±0.10
.02	.86	.02	2.45±0.09	-0.02±0.06	0.06±0.03
			-0.55±0.11	1.80±0.10	-0.61±0.28
			0.11±0.07	0.06±0.04	2.04±0.07
.86	.02	.02	1.28±0.10	-0.44±0.08	-0.51±0.10
			0.06±0.04	1.81±0.13	-0.01±0.06
			0.04±0.07	-0.08±0.06	1.33±0.09

As may be seen from Table 1 the errors given for the main diffusion coefficients range from about two to six percent, whereas some of the errors for the cross terms are as high as 300 percent. Also, it is probable that the actual errors are greater than those given since the three calculations used to determine the errors were not completely independent. The large percentage errors in the cross terms are due to the small magnitude of the cross terms in relation to the main terms.

Since no data has been published for diffusion in a four component system, it was impossible to confirm the validity of the experimental technique and the data analysis with respect to previous work. Methods have been presented, however, for the prediction of multicomponent diffusivities based upon binary diffusion data and thermodynamic data. Alimadadian (2) has presented such a method which is based upon a modification of absolute rate theory in conjunction with a lattice structured model for the liquid state. This method was shown to be capable of predicting the main diffusion coefficients in three ternary systems with an average error of 7.5 percent.

In Table 2 the main diffusion coefficients determined in this work are compared with the predictions calculated using Alimadadian's method. In making the predictions, the activities of the components were assumed to be equal to their mole fractions. For about half of the main

TABLE 2

COMPARISON OF EXPERIMENTAL MAIN DIFFUSION
COEFFICIENTS WITH PREDICTED VALUES

Weight Fractions				Main Diffusion Coefficients (Cm ² /Sec)		
W ₁	W ₂	W ₃		D ₁₁ x10 ⁵	D ₂₂ x10 ⁵	D ₃₃ x10 ⁵
.25	.25	.25	experimental	1.94±0.05	1.98±0.06	1.73±0.09
			predicted	2.01	2.13	1.65
.20	.30	.40	experimental	2.11±0.12	1.99±0.08	1.86±0.11
			predicted	2.35	2.10	1.74
.30	.30	.30	experimental	1.84±0.08	1.79±0.12	1.65±0.06
			predicted	1.88	2.03	1.57
.15	.15	.60	experimental	2.44±0.14	2.70±0.10	1.92±0.06
			predicted	2.30	2.77	1.91
.15	.60	.15	experimental	2.01±0.09	1.83±0.04	1.93±0.11
			predicted	1.85	1.90	2.04
.60	.15	.15	experimental	1.55±0.16	1.71±0.09	1.62±0.11
			predicted	1.62	1.67	1.73
.44	.44	.02	experimental	1.59±0.07	1.77±0.11	1.49±0.09
			predicted	1.66	1.89	1.42

TABLE 2 (CONTINUED)

COMPARISON OF EXPERIMENTAL MAIN DIFFUSION
COEFFICIENTS WITH PREDICTED VALUES

Weight Fractions			Main Diffusion Coefficients (Cm ² /Sec)			
W ₁	W ₂	W ₃		D ₁₁ x10 ⁵	D ₂₂ x10 ⁵	D ₃₃ x10 ⁵
.44	.02	.44	experimental	2.06±0.04	2.27±0.09	1.76±0.14
			predicted	2.00	2.38	1.60
.02	.44	.44	experimental	3.01±0.22	2.30±0.09	2.33±0.10
			predicted	2.47	2.27	2.20
.02	.86	.02	experimental	2.45±0.09	1.80±0.10	2.04±0.07
			predicted	2.52	2.03	1.95
.86	.02	.02	experimental	1.28±0.10	1.81±0.13	1.33±0.09
			predicted	1.40	1.77	1.36

diffusion coefficients in Table 2 the predicted value lies within the experimentally determined range. If the probable error in the predictive technique based upon ternary data is taken into account, the range of prediction overlaps the experimental range in every case except one. Because of the large errors in the cross term diffusion coefficients as well as the probability of large errors in predicting these terms, no comparison of the experimental and predicted values was attempted.

In order to use the predictive techniques developed by Alimadadian, values of infinite dilution binary diffusion coefficients are required. These binary diffusivities were measured at 25°C for every combination of the components used in the quarternary study. The results of these experiments are presented in Table 3.

TABLE 3

BINARY INFINITE DILUTION DIFFUSION

DATA AT 25°C

Solvent	Solute	$D \times 10^5$, (Cm ² /Sec)
n-decane	toluene	2.12
n-decane	n-heptane	1.79
n-decane	cyclohexane	1.94
toluene	n-decane	1.58
toluene	n-heptane	2.20
toluene	cyclohexane	2.39
n-heptane	toluene	3.70
n-heptane	n-decane	2.55
n-heptane	cyclohexane	3.58
cyclohexane	toluene	1.57
cyclohexane	n-decane	0.941
cyclohexane	n-heptane	1.22

CHAPTER III

PREDICTION OF MULTICOMPONENT DIFFUSION COEFFICIENTS

Background

Because of the complexity of the liquid state and the diffusion process, no rigorous theory for the prediction of diffusion coefficients in liquids has been possible to this time. This is especially true for multicomponent systems because of the coupling effect between the molecular fluxes. Available methods for the prediction of multicomponent diffusivities rely on semi-empirical models of the liquid state. Most of the methods depend upon the use of diffusion data for the binary systems formed from the components of the multicomponent system and upon multicomponent thermodynamic data.

Two models have provided the basis for most of the effort in predicting multicomponent diffusion coefficients. The first model is based upon the hydrodynamic theory developed by Einstein (22, 23, 24, 25) and Sutherland (48). In this theory, diffusional flow is regarded as a balance

between a driving force which is the gradient of chemical potential and a viscous resistance to flow. Cussler and Lightfoot (13) were the first to apply the hydrodynamic theory to multicomponent solutions. Others who have used this model for the basis of their predictive techniques include Furlong (29) and Kett (37). Each of these methods has been proven reasonably accurate in predicting ternary diffusion coefficients for selected systems, although the data required for their use is often not available.

The second model used in the predictive techniques is based upon the absolute rate theory developed by Eyring and co-workers. In this theory diffusion occurs through a series of jumps over a free energy barrier. The length of the jumps is governed by a lattice model of the liquid which has sites separated by a distance on the order of the molecular diameters. The presence of a driving force is assumed to reduce the activation energy required for a forward jump while increasing it for a jump in the opposite direction. Workers who have used modifications of the absolute rate theory for the prediction of multicomponent diffusion coefficients include Cullinan and Cusick (10), Lane and Kirkaldy (39) and Alimadadian (2).

The most promising method for the development of a rigorous theory of diffusion is through statistical mechanical investigations. Such a development is not presently possible because of a lack of knowledge of intermolecular potentials

and particle distribution functions. It has been possible, however, to use the statistical mechanical approach to describe diffusion in a hypothetical mixture of rigid spheres. The development of such theories by Enskog (8) and others has provided much insight into the analysis of experimental data. The analysis of diffusion in a pure fluid by Enskog has been extended to the binary case by Thorne (15) and to the general multicomponent case by Tham and Gubbins (50).

In the following sections a method of prediction of multicomponent diffusion coefficients, based upon the rigid sphere model, will be developed. Tham and Gubbins (50) have shown that the rigid sphere model is able to qualitatively predict diffusion behavior in a multicomponent solution. It is not expected, however, that such a model would give good quantitative results, since real fluids are not composed of rigid spheres. Since the principal independent variables in the rigid sphere model are molecular diameters and masses, it is proposed that a predictive technique for multicomponent diffusivities may be developed by empirically varying these parameters within the framework of the model. A continuous association model will be used to describe the effective size of the component molecules.

Equation Development

The general equations giving multicomponent diffusion coefficients in a rigid sphere fluid have been derived

by Tam and Gubbins (50). The basic equation may be given in matrix form as

$$D = F^{-1} Z M^{-1} \quad (44)$$

The matrix M is the diagonal matrix of order N-1 with the masses of the component molecules on the main diagonal.

The elements of the matrix F are given by the following equation.

$$F_{ij} = - \sum_{\ell=1}^N \frac{n_i n_\ell g_{i\ell} \delta_{ij}}{n_j n_{i\ell} \mathcal{D}_{ij}} (M_j M_i)^{-\frac{1}{2}} + \frac{n_i g_{ij}}{M_j n_{i\ell} \mathcal{D}_{ij}} \\ + \sum_{\ell=1}^N \frac{n_i n_\ell g_{ij}}{n_N n_{i\ell} \mathcal{D}_{i\ell}} (M_N M_\ell)^{-\frac{1}{2}} \left[\left(\frac{M_\ell}{M_i} \right)^{\frac{1}{2}} \delta_{iN} - \delta_{\ell N} \right] \quad (45)$$

where N_i is the number density of component i , M_i is the mass of a molecule of component i , g_{ij} is the radial distribution function evaluated at σ_{ij} , \mathcal{D}_{ij} is the dilute gas binary diffusion coefficient, and δ_{ij} is the Kronecker delta. The matrix Z in Eq. (44) is composed of the elements

$$Z_{ij} = E_{iN} (P_j/P_N) - E_{ij} \quad (46)$$

where the P's and E's are terms describing interactions between the species and are given by

$$E_{ij} = \delta_{ij} + 2\rho b_{ji} g_{ij} + \sum_{\ell} n_i \rho b_{i\ell} \frac{\partial g_{i\ell}}{\partial n_j} \quad (47)$$

and

$$P_i = \sum_j \left[\delta_{ij} + 2\rho b_{ij} g_{ji} + \sum_l n_j \rho b_{jl} \frac{\partial g_{jl}}{\partial n_i} \right] = \sum_j E_{ji} \quad (48)$$

The term ρb_{ij} may be given in terms of reduced variables as

$$\rho b_{ij} = \xi X_j (R_i + R_j)^3 / 2Y_N \quad (49)$$

where X_j is the mole fraction of component j , ξ is the reduced density given by

$$\xi = \frac{1}{6} \pi \sum_{i=1}^N n_i \sigma_{ii}^3 \quad (50)$$

where σ_{ii} is the molecular diameter of component i , the R 's are reduced diameters, and the term Y_i is given by

$$Y_i = \sum_{j=1}^N X_j R_j^i \quad (51)$$

The dilute gas binary diffusion coefficient may be given in terms of these reduced variables as

$$n^0_{ij} = \left[\frac{3}{2\sigma_{NN}^2} \left(\frac{kT}{2\pi M_3} \right)^{\frac{1}{2}} \right] \frac{1}{(R_i + R_j)^2} \left(\frac{\bar{M}_i + \bar{M}_j}{\bar{M}_i \bar{M}_j} \right)^{\frac{1}{2}} \quad (52)$$

where k is Boltzman's constant, T is temperature in $^{\circ}K$, and \bar{M}_i is the reduced molecular weight of component i . Carnahan and Starling (7) have presented an equation for the radial distribution function for a fluid composed of rigid spheres which is accurate up to a reduced density of about 0.52,

$$g_{ij} = \frac{1}{1-\xi} + \frac{3\xi}{(1-\xi)^2} \left[\frac{R_i R_j}{(R_i + R_j)} \right] \frac{Y_2}{Y_3} + \frac{2\xi^2}{(1-\xi)^3} \left[\frac{R_i R_j}{(R_i + R_j)} \right]^2 \left(\frac{Y_2}{Y_3} \right)^2 \quad (53)$$

The preceding group of equations allows computation of the multicomponent diffusivities for a rigid sphere fluid. The only data needed to carry out the computations are the mole fractions, molecular weights, molecular diameters, and number densities of each component.

For binary systems the calculation of the diffusion coefficient is greatly simplified and may be given by the following equation

$$D_{ij} = (P_2 E_{11} - P_1 E_{12}) / (n_i P_1 + n_j P_2) (n_{ij}^\infty / g_{ij}) \quad (54)$$

where the same definitions apply as for the multicomponent case. If one component is infinitely dilute Eq. (54) reduces to

$$D_{ij}^\infty = n_{ij}^\infty / n_j g_{ij}^\infty \quad (55)$$

As mentioned previously, the above analysis is not able to give good quantitative results for diffusion in real multicomponent solutions. Therefore the technique is empirically modified to conform with observed behavior. The diameters of the constituent species are calculated from

known values of self diffusion coefficients or from infinite dilution diffusion coefficients in a fluid whose diameter is known. This calculation is performed by varying the value of the molecular diameter until the diffusivity predicted by Eq. (55) agrees with the experimental value. This procedure yields a rigid sphere diameter which will simulate real diffusion behavior.

The rigid sphere model does not take into account attractive forces between molecules, tendencies of molecules to associate with one another, or other factors which may affect the motion of the molecules. In order to compensate for these shortcomings a continuous association model similar to that described by Prigogine and Defay (44) will be superimposed upon the rigid sphere diffusion model. Although all molecules do not necessarily form real associations with other species in the solution, it will be assumed that this model holds in order to empirically describe a real system.

It is assumed that all degrees of association consisting of two different types of molecules are possible within the solution and that the number density of a particular species may be given by a relation of the form

$$n_{A_j B_k} = n_{A_1}^j n_{B_1}^k K_{AB}^{j+k-1} \quad (56)$$

where A and B refer to particular components and j and k refer to the number of monomers of the species. The term K_{AB} is

the association constant for the species A and B. Thus the number density of any species $A_i B_j$ may be determined if n_{A_1} , n_{B_1} (the number densities of the monomers), and K_{AB} are known. For a ternary system with components A, B, and C the total number density of A is given as follows

$$n_A^T = \sum_{i=1}^{\infty} i \cdot n_{A_i} + \sum_{i=1}^{\infty} \sum_{j=1}^{\infty} i \cdot n_{A_i B_j} + \sum_{i=1}^{\infty} \sum_{j=1}^{\infty} i \cdot n_{A_i C_j} \quad (57)$$

By using Eq. (56) to replace the terms n_{A_i} , $n_{A_i B_j}$, and $n_{A_i C_j}$, Eq. (57) may be reduced to

$$n_A^T = \frac{n_{A_1}}{(1 - K_A n_{A_1})^2} + \frac{n_{A_1} K_{AB} n_{B_1}}{(1 - K_{AB} n_{A_1})^2 (1 - K_{AB} n_{B_1})} + \frac{n_{A_1} K_{AC} n_{C_1}}{(1 - K_{AC} n_{A_1})^2 (1 - K_{AC} n_{C_1})} \quad (58)$$

Equations similar to Eq. (58) may be derived for n_B^T and n_C^T . These three equations may be solved for n_{A_1} , n_{B_1} , and n_{C_1} by using the method of successive substitutions. Rearranging Eq. (58) yields

$$n_{A_1} = (1 - K_A n_{A_1})^2 \left[n_A^T - \frac{n_{A_1} K_{AB} n_{B_1}}{(1 - K_{AB} n_{A_1})^2 (1 - K_{AB} n_{B_1})} - \frac{n_{A_1} K_{AC} n_{C_1}}{(1 - K_{AC} n_{A_1})^2 (1 - K_{AC} n_{C_1})} \right] \quad (59)$$

By substituting estimates for n_{A_1} , n_{B_1} , and n_{C_1} into the right side of Eq. (59) an improved value for n_{A_1} is calculated. Corresponding equations for n_{B_1} and n_{C_1} allow calculations of improved values of these terms. These equations form the basis for an iterative scheme which was found to converge rapidly when the values of the association constants were less than about .5. This method is easily extended to systems with more than three components.

The object of using the continuous association model is to be able to calculate the average properties of the components of the solution. Since some species of the solution are composed of monomers of different species, the question arises as to how the averages may be calculated. It was arbitrarily decided to allow the effect of a species $A_i B_j$ upon the average properties of A to be weighted by the ratio of the number of A monomers to the total number of monomers in the species. Thus the average molecular weight of component A in a ternary system may be given by

$$\begin{aligned} \bar{M}_A = & \sum_{i=1}^{\infty} \frac{n_{A_i}}{n_A^T} \cdot i \cdot M_A + \sum_{i=1}^{\infty} \sum_{j=1}^{\infty} \frac{n_{A_i B_j}}{n_A^T} \left(\frac{i}{i+j}\right) (i \cdot M_A + j \cdot M_B) \\ & + \sum_{i=1}^{\infty} \sum_{j=1}^{\infty} \frac{n_{A_i C_j}}{n_A^T} \left(\frac{i}{i+j}\right) (i \cdot M_A + j \cdot M_C) \end{aligned} \quad (60)$$

To calculate the average diameters it is assumed that the volumes of the associated species are additive, or

$$\left(\sigma_{A_i B_j}\right)^3 = i \cdot \sigma_{A_1}^3 + j \cdot \sigma_{B_1}^3 \quad (61)$$

Therefore the average molecular diameter of component A is

$$\begin{aligned} \bar{\sigma}_A = & \left[\sum_{i=1}^{\infty} \frac{n_{A_i}}{n_A^T} \cdot i \cdot \sigma_{A_1}^3 + \sum_{i=1}^{\infty} \sum_{j=1}^{\infty} \frac{n_{A_i B_j}}{n_A^T} \left(\frac{i}{i+j}\right) \left(i \cdot \sigma_{A_1}^3 + j \cdot \sigma_{B_1}^3\right) \right. \\ & \left. + \sum_{i=1}^{\infty} \sum_{j=1}^{\infty} \frac{n_{A_i C_j}}{n_A^T} \left(\frac{i}{i+j}\right) \left(i \cdot \sigma_{A_1}^3 + j \cdot \sigma_{C_1}^3\right) \right]^{1/3} \end{aligned} \quad (62)$$

Analogous expressions are used to find the average molecular weights of components B and C.

The determination of the association constants is based upon use of the infinite dilution binary diffusion coefficients. To calculate the value of the constant K_{AB} a trial value is first assumed. It is then possible to calculate the average properties of a binary mixture of A and B in which one component is infinitely dilute. Equation (55)

is then used to determine the value of the infinite dilution diffusion coefficient. The value of the association constant is changed until the calculated diffusion coefficient agrees with the experimental value. In practice this procedure was facilitated through use of the golden section search algorithm.

The value determined for K_{AB} will in general vary depending upon whether D_{AB}^{∞} or D_{BA}^{∞} was used in the calculation. If K_{AB_1} and K_{AB_2} are used to denote these two calculations then the value of K_{AB} which was used in the final calculation may be given by

$$K_{AB} = (X_A \cdot K_{AB_1} + X_B \cdot K_{AB_2}) / (X_A + X_B) \quad (63)$$

The preceding paragraphs have outlined the calculations necessary for the prediction of multicomponent diffusion coefficients. The data necessary for this procedure include molecular weights, mole fractions, self and infinite dilution diffusion coefficients, and the temperature. The steps in the calculational procedure may be summarized by the following list:

1. Determine values of monomer diameters from self or infinite dilution diffusion data.
2. Determine values of association constants from infinite dilution diffusion coefficients.

3. Calculate average properties for each component at its particular concentration.
4. Use the rigid sphere diffusion model to predict the multicomponent diffusivities.

Comparison with Experimental Data

The predictive technique developed in this chapter was tested against data for three systems. The first system used was the quaternary system experimentally studied in this work. Table 4 gives the results of the technique and the experimental data for the main diffusion coefficients. No attempt was made to compare the results for the cross-terms for this system. Table 5 presents a comparison of the experimental data of Shuck and Toor (46) for the ternary system methanol-iso-butanol-n-propanol at 30°C with the predicted diffusivities. A similar comparison for the data of Cullinan and Toor (11) for the system acetone-benzene-carbon tetrachloride is given in Table 6.

It may be seen that the predictive technique is able to predict multicomponent diffusivities with moderate accuracy. For the data in Tables 5 and 6 it may be noted that although the sign of the predicted cross-terms is correct in most cases, the magnitudes of these terms is generally too small. Thus, the technique seems to predict coupling effects which are less than those experimentally observed.

TABLE 4

COMPARISON OF MAIN DIFFUSION COEFFICIENTS FOR
 THE SYSTEM CYCLOHEXANE (1) - TOLUENE (2) -
 n-HEPTANE (3) - n-DECANE (4) WITH
 PREDICTED VALUES

Weight Fractions			Diffusion Coefficients (Cm ² /Sec)			
W ₁	W ₂	W ₃		D ₁₁ x10 ⁵	D ₂₂ x10 ⁵	D ₃₃ x10 ⁵
.25	.25	.25	expt.	1.94	1.98	1.73
			calc.	2.13	2.27	1.62
.20	.30	.40	expt.	2.11	1.99	1.86
			calc.	2.20	2.16	1.79
.30	.30	.30	expt.	1.84	1.79	1.65
			calc.	1.93	1.98	1.48
.15	.15	.60	expt.	2.44	2.70	1.92
			calc.	2.52	2.61	1.80
.15	.60	.15	expt.	2.01	1.83	1.93
			calc.	2.05	1.92	2.02
.60	.15	.15	expt.	1.55	1.71	1.62
			calc.	1.68	1.80	1.55
.44	.44	.02	expt.	1.59	1.77	1.49
			calc.	1.63	1.86	1.57
.44	.02	.44	expt.	2.06	2.27	1.76
			calc.	2.38	2.20	1.82
.02	.44	.44	expt.	3.01	2.30	2.33
			calc.	2.65	2.43	2.28
.02	.86	.02	expt.	2.45	1.80	2.04
			calc.	2.55	1.82	2.13
.86	.02	.02	expt.	1.28	1.81	1.33
			calc.	1.37	1.69	1.29

TABLE 5

COMPARISON OF EXPERIMENTAL DIFFUSION COEFFICIENTS FOR THE
 SYSTEM METHANOL(1) - ISO-BUTANOL(2) - n-PROPANOL(3)
 WITH PREDICTED VALUES

Mole Fractions		Diffusion Coefficients (Cm ² /Sec)				
X ₁	X ₂		D ₁₁ x10 ⁵	D ₁₂ x10 ⁵	D ₂₁ x10 ⁵	D ₂₂ x10 ⁵
0.460	0.240	expt.	1.039	0.032	-0.023	0.875
		calc.	1.162	0.021	-0.014	0.932
0.250	0.100	expt.	0.909	0.030	-0.009	0.721
		calc.	0.977	0.016	0.002	0.810
0.270	0.570	expt.	0.765	0.027	-0.039	0.624
		calc.	0.704	0.011	-0.014	0.610
0.820	0.070	expt.	1.505	0.211	-0.004	1.383
		calc.	1.722	0.113	0.011	1.307

TABLE 6

COMPARISON OF EXPERIMENTAL DIFFUSION COEFFICIENTS FOR THE
 SYSTEM ACETONE(1) - BENZENE(2) - CARBON
 TETRACHLORIDE(3) WITH PREDICTED VALUES

Mole Fractions		Diffusion Coefficients (Cm ² /Sec)				
X ₁	X ₂		D ₁₁ ×10 ⁵	D ₁₂ ×10 ⁵	D ₂₁ ×10 ⁵	D ₂₂ ×10 ⁵
0.300	0.350	expt.	1.887	-0.213	-0.037	2.225
		calc.	1.753	-0.174	-0.012	2.134
0.150	0.150	expt.	1.598	-0.058	-0.083	1.812
		calc.	1.673	-0.041	-0.009	1.743
0.150	0.700	expt.	1.853	0.049	-0.068	1.841
		calc.	1.944	0.031	-0.019	1.902
0.700	0.150	expt.	2.132	0.051	-0.071	2.062
		calc.	2.054	0.006	-0.043	2.044

CHAPTER IV

CONCLUSIONS AND RECOMMENDATIONS

From the results of this study it can be concluded that the diffusion coefficients for a four component liquid system may be measured using an experimental apparatus composed of a flowing junction diffusion cell and a birefringent interferometer. Although the accuracy of the measurements for the four component system studied does not approach that obtainables for ternary or binary systems, the determined diffusion coefficients are adequate for many engineering purposes. Possible methods to improve the accuracy of the diffusion coefficients include refinements in the optical system of the interferometer to reduce the width of the interference fringes, and changes in the data to allow the use of more than three runs for each determination. It is recommended that a detailed error analysis be performed on the experimental procedure and the data analysis in order to determine the most significant error producing factors.

Because of the small magnitude and the relative error of the cross-term diffusion coefficients measured in

this study, it was not possible to perform a meaningful test of the Onsager Reciprocal Relations. It is recommended that an experimental study be carried out on a system in which the cross-term diffusion coefficients might be expected to be larger.

The rigid sphere model for diffusion in a multi-component liquid solution has been shown to be a useful basis for the prediction of multicomponent diffusivities. The use of empirically determined parameters found through application of a continuous association model allows the rigid sphere model to predict multicomponent diffusivities with moderate accuracy. The principal advantage of this method is that thermodynamic data is not required for its application. This is fortunate since multicomponent thermodynamic data is probably even more difficult to obtain than diffusion data, and it is usually necessary to resort to approximations based upon binary thermodynamic data. The main objection to the developed predictive technique is probably its complexity. Once the procedure has been programmed for a digital computer, however, the required data is fairly simple and in most cases obtainable. Further work is necessary in order to simplify the technique and put it in a more tractable form. It is also recommended that a study be made of the effect of other association models on the predictive technique.

LITERATURE CITED

1. Albright, J.G. and R. Mills, J. Phys. Chem., 69, 3120 (1965).
2. Alimadadian, A., Ph.D. Dissertation, University of Oklahoma, Norman, Oklahoma (1971).
3. Baldwin, R.L., P.J. Dunlop and L.J. Gosting, J. Amer. Chem. Soc., 77, 5235 (1955).
4. Bearman, R.J., J. Chem. Phys., 32, 1308 (1960).
5. Bryngdahl, O., Acta. Chem. Scand., 11, 1017 (1957).
6. Burchard, J.K. and H.L. Toor, J. Phys. Chem., 66, 2015 (1962).
7. Carnahan, N.F. and K.E. Starling, J. Chem. Phys., 51, 635 (1969).
8. Chapman, S. and T.G. Cowling, The Mathematical Theory of Non-Uniform Gases, Cambridge University, Cambridge (1952).
9. Cullinan, H.T., Masters Thesis, Carnegie Inst. of Technology, Pittsburgh, Pennsylvania (1963).
10. Cullinan, H.T. and M.R. Cusick, Ind. Eng. Chem. Fund., 6, 72 (1967).
11. Cullinan, H.T., Jr. and H.L. Toor, J. Phys. Chem., 69, 3941 (1965).
12. Cussler, E.L., Ph.D. Dissertation, University of Wisconsin, Madison, Wisconsin (1965).
13. Cussler, E.L. and E.N. Lightfoot, J. Phys. Chem., 69, 2875 (1965).
14. DeGroot, S.R. and P. Mazur, Non-Equilibrium Thermodynamics, North-Holland Publishing Company, Amsterdam (1962).

15. Dunlop, P.J., J. Phys. Chem., 61, 994 (1957).
16. Dunlop, P.J., J. Phys. Chem., 61, 1619 (1957).
17. Dunlop, P.J., J. Phys. Chem., 63, 612 (1959).
18. Dunlop, P.J., J. Phys. Chem., 69, 4276 (1965).
19. Dunlop, P.J. and L.J. Gosting, J. Amer. Chem. Soc., 77, 5238 (1955).
20. Dunlop, P.J. and L.J. Gosting, J. Phys. Chem., 63, 86 (1959).
21. Dunlop, P.J. and L.J. Gosting, J. Phys. Chem., 68, 3874 (1964).
22. Einstein, A., Ann. Physik, LPZ., 17, 549 (1905).
23. Einstein, A., Ann. Physik, LPZ., 19, 371 (1906).
24. Einstein, A., Investigation on the Theory of the Brownian Movement, Meuten and Company, London (1926).
25. Einstein, A., Z. Electrochem., 14, 235 (1908).
26. Ellerton, H.D. and P.J. Dunlop, J. Phys. Chem., 71, 1291 (1967).
27. Fick, A., Ann. Physik, 94, 59 (1855).
28. Fujita, H. and L.J. Gosting, J. Phys. Chem., 64, 1256 (1960).
29. Furlong, L.E., Ph.D. Dissertation, University of Wisconsin, Madison, Wisconsin (1968).
30. Graff, R.A. and T.B. Drew, Ind. Eng. Chem. Fund., 1, 490 (1968).
31. Glasstone, S., K. Laidler and H. Eyring, The Theory of Rate Processes, McGraw Hil, New York (1941).
32. Haluska, J.L., Ph.D. Dissertation, University of Oklahoma, Norman, Oklahoma (1970).
33. Hirschfelder, J.O., C.F. Curtiss and R.B. Bird, Molecular Theory of Gases and Liquids, Wiley, New York (1954).
34. Holmes, J.J., D.R. Olander and C.R. Wilke, A.I.Ch.E. J., 8, 646 (1962).

35. Hooke, R. and T.A. Jeeves, J. Assoc. Comp. Mach., 8, 212 (1961).
36. Kelly, F.J., Diffusion and Viscosity in Three-Component Systems, University of New England, Armidale, N.S.W., Australia (1961).
37. Kett, T.K., Ph.D. Dissertation, Michigan State University, East Lansing, Michigan (1968).
38. Laidler, K.J., Reaction Kinetics, Pergamon Press, New York (1963).
39. Lane, J.E. and J.S. Kirkaldy, Can. J. Chem., 43, 1812 (1965).
40. Merliss, F.E., Ph.D. Dissertation, University of Oklahoma, Norman, Oklahoma (1967).
41. Onsager, L., Ann. N.Y. Acad. Sci., 46, 241 (1945).
42. Onsager, L., Phys. Rev., 37, 405 (1931); 38, 2265 (1931).
43. Onsager, L., Ann. N.Y. Acad. of Sci., 34, 930 (1948).
44. Prigogine, I. and R. Defay, Chemical Thermodynamics, Wiley, New York (1962).
45. Reinfelds, G. and L.J. Gosting, J. Phys. Chem., 68, 2464 (1964).
46. Shuck, F.O. and H.C. Toor, J. Phys. Chem., 67, 540 (1963).
47. Skinner, R.D., Masters Thesis, Oklahoma State University, Stillwater, Oklahoma (1964).
48. Sutherland, W., Phil. Mag., 9, 781 (1903).
49. Svensson, H., Acta. Chem. Scand., 3, 1170 (1949).
50. Tham, M.K. and K.E. Gubbins, J. Chem. Phys., 55, 268 (1971).
51. Vadovic, C.J., Ph.D. Dissertation, University of Oklahoma, Norman, Oklahoma (1972).
52. Weir, F.E. and M. Dole, J. Amer. Chem. Soc., 80, 302 (1958).
53. Wendt, R.P., J. Phys. Chem., 66, 1279 (1962).

54. Woolf, L.A., J. Phys. Chem., 67, 273 (1963).
55. Woolf, L.A., D.G. Miller and L.J. Gosting, J. Amer. Chem. Soc., 84, 317 (1962).

NOMENCLATURE

A	Area under concentration gradient curve
C_i	Concentration of component i
\bar{C}	Average concentration
\hat{C}	Modified concentration vector
ΔC	Concentration increment
D_{ij}	Multicomponent diffusion coefficient
DA	Reduced height to area ratio
DM	Reduced first moment
DS	Reduced second moment
g_{ij}	Radial distribution function
h	Height of concentration gradient curve
J_i	Diffusional flux of species i
K	Association constant
k	Boltzmann's constant
L_{ij}	Phenomenological coefficient
M	Modal matrix of diffusivity matrix
\bar{M}	Reduced molecular weight
N	Number of components
n	Refractive index

\bar{n}	Refractive index at concentration \bar{C}
n_i	Number density of component i
Δn	Total difference in refractive index
n_{ij}^0	Dilute gas binary diffusion coefficient
P_i	Defined variable, Eq. (18)
Q	Minimization variable
R_i	Derivative of refractive index with respect to C
S	Second semi-moment
T	Temperature
T_i	Defined variable, Eq. (38)
t	Time
t_0	Zero time correction
W	Width of concentration gradient curve
W_i	Weight fraction of component i
X	Length in direction of diffusion
X_i	Mole fraction of component i
Y_i	Thermodynamic driving force
Z	Optical path length
α	Length of diffusion cell
δ_{ij}	Kronecker delta
λ_i	Eigenvalue of diffusivity matrix
ξ	Reduced density
σ_{ii}	Molecular diameter

APPENDIX A

Solution of Differential Equations for Multicomponent Diffusion

Fick's second law of diffusion may be extended to the multicomponent case (1) and written as follows in matrix form

$$\frac{\partial C}{\partial t} = D \frac{\partial^2 C}{\partial X^2} \quad (A1)$$

where C is the concentration vector and D is the matrix of diffusion coefficients. Both C and D are of order $N-1$ for a N component system. For the experimental geometry used in this work the following boundary conditions apply,

$$C = \bar{C} + \frac{\Delta C}{2} \text{ for } X > 0, t=0 \quad (A2)$$

$$C = \bar{C} - \frac{\Delta C}{2} \text{ for } X < 0, t=0 \quad (A3)$$

$$C \rightarrow \bar{C} + \frac{\Delta C}{2} \text{ for } X \rightarrow \infty, t>0 \quad (A4)$$

$$C \rightarrow \bar{C} - \frac{\Delta C}{2} \text{ for } X \rightarrow -\infty, t>0 \quad (A5)$$

where \bar{C} is the mean concentration vector and ΔC is the vector of concentration differences between the top and bottom solutions.

Define the matrices M and \hat{C} such that

$$C = M \hat{C} \quad (A6)$$

and M is the modal matrix of the matrix D (i.e., the column vectors of M are eigenvectors of D).

Substitution of Eq. (A6) in Eq. (A1) and premultiplication by M^{-1} yields

$$M^{-1}M \frac{\partial \hat{C}}{\partial t} = [M^{-1}DM] \frac{\partial^2 \hat{C}}{\partial t^2} \quad (A7)$$

Since the quantity in brackets reduces to the vector of eigenvalues of the D matrix, Eq. (A7) may be written as

$$\frac{\partial \hat{C}}{\partial t} = \lambda \frac{\partial^2 \hat{C}}{\partial t^2} \quad (A8)$$

where λ is the vector of eigenvalues of D .

The partial differential equation, Eq. (A8) may be transformed to an ordinary differential equation by using a similarity transformation defined as

$$\eta_i = \frac{x}{2\sqrt{\lambda_i t}} \quad (A9)$$

Application of this transformation yields

$$-2\eta \frac{dC}{d\eta} = \frac{d^2 \hat{C}}{d\eta^2} \quad (A10)$$

with the following transformed boundary conditions,

$$\hat{C}(\infty) = M^{-1}(\bar{C} + \frac{\Delta C}{2}) \text{ for } \eta \rightarrow \infty \quad (\text{A11})$$

$$\hat{C}(-\infty) = M^{-1}(\bar{C} - \frac{\Delta C}{2}) \text{ for } \eta \rightarrow -\infty \quad (\text{A12})$$

Integration of Eq. (A10) yields

$$\frac{\hat{C}(\eta) - \hat{C}(-\infty)}{\hat{C}(\infty) - \hat{C}(-\infty)} = \frac{1}{2} \{1 + \text{erf}(\eta)\} \quad (\text{A13})$$

or

$$\hat{C}(\eta) = \frac{1}{2}(\hat{C}(\infty) - \hat{C}(-\infty)) + \frac{1}{2}(\hat{C}(\infty) + \hat{C}(-\infty)) \text{erf}(\eta) \quad (\text{A14})$$

The vector of concentrations may then be found through application of Eq. (A6).

For a ternary system the elements of the modal matrix may be evaluated and substituted in Eq. (A14). (2) The result of this operation is

$$\begin{aligned} C_1 - \bar{C}_1 = & \frac{1}{2} \left\{ \left(\frac{\lambda_2 - D_{11}}{\lambda_2 - \lambda_1} \right) \Delta C_1 - \frac{D_{12}}{\lambda_2 - \lambda_1} \Delta C_2 \right\} \text{erf}(\eta_1) \\ & + \frac{1}{2} \left\{ - \left(\frac{\lambda_1 - D_{11}}{\lambda_2 - \lambda_1} \right) \Delta C_1 - \frac{D_{12}}{\lambda_2 - \lambda_1} \Delta C_2 \right\} \text{erf}(\eta_2) \end{aligned} \quad (\text{A15})$$

$$\begin{aligned} C_2 - \bar{C}_2 = & \frac{1}{2} \left\{ \frac{(\lambda_2 - D_{11})(\lambda_1 - D_{11})}{D_{12}(\lambda_2 - \lambda_1)} \Delta C_1 - \frac{D_{12}}{(\lambda_2 - \lambda_1)} \Delta C_2 \right\} \text{erf}(\eta_1) \\ & + \frac{1}{2} \left\{ - \frac{(\lambda_2 - D_{11})(\lambda_1 - D_{11})}{D_{12}(\lambda_2 - \lambda_1)} \Delta C_1 \right. \\ & \left. + \frac{(\lambda_2 - D_{11})}{(\lambda_2 - \lambda_1)} \Delta C_2 \right\} \text{erf}(\eta_2) \end{aligned} \quad (\text{A16})$$

For systems of order greater than three, equations of the form of (A15) and (A16) become too cumbersome and the most practical solution is in the form of Eq. (A14).

APPENDIX B

Chemical Specifications

A. Toluene		
Freezing point purity, mole percent		99.9
Specific gravity, 60/60		0.8720
Composition, wt. percent by GLC		
Toluene		99.9+
Unidentified		Trace
B. Normal Heptane		
Purity, mole percent		99.7
Boiling point, 760 mmHg, °C		98.
Density at 20°C, g/ml		.68383
Refractive index, n _D ²⁰		1.38770
C. Cyclohexane		
Freezing point purity, mole percent		99.8
Color, Saybolt		+30
Composition, wt. percent by GLC		
Cyclohexane		99.9+
D. Normal Decane		
Freezing point purity, mole percent		99.6
Composition, wt. percent by GLC		
n-Decane		99.9+
Unidentified		Trace

APPENDIX C

Binary Data Analysis

The mathematical analysis of binary diffusion data is based on Fick's second law, with the boundary conditions associated with free diffusion in one direction and a step function in concentration at the start of an experiment.

The solution of Fick's equation for this case is

$$\frac{C_A - C_{AO}}{C_{A1} - C_{AO}} = \frac{1}{2} \left[1 + \operatorname{erf} \left(\frac{X}{\sqrt{4D_{AB}t}} \right) \right] \quad (C1)$$

where C_{AO} and C_{A1} refer to the concentrations at the ends of the diffusion cell. The optical path length is assumed to be a linear function of concentration as follows,

$$z = \alpha n = \alpha [n_0 + n_1 (C_A - C_{AO})] \quad (C2)$$

Substituting C_A from Eq. (C1) into Eq. (C2) and differentiating with respect to X yields

$$\frac{\partial z}{\partial X} = \frac{z_1 - z_0}{2 \sqrt{\pi D_{AB}t}} \exp \left(\frac{-(2X)^2}{16 D_{AB}t} \right) \quad (C3)$$

This equation describes the fringe patterns which are

recorded during an experimental run. The maximum of the optical path gradient curve occurs at $X=0$, thus

$$\left(\frac{\partial Z}{\partial X}\right)_{\max} = \frac{Z_1 - Z_0}{2 \sqrt{\pi D_{AB} t}} \quad (C4)$$

Previous methods of data analysis for this system involved measurement of the width of the curve at a constant level of the optical path gradient. These measurements were then used in a non-linear least squares analysis to determine the diffusion coefficient and the maximum width of the curve at the level of the measurements. The disadvantages of this method were that only one point on each curve was utilized, and the determination of the same level of the optical path gradient on each photograph was difficult. Also, the analysis required an iterative type calculation.

An improved method of analysis may be developed by considering the ratio of the height of the curve to the maximum height at several points on each curve, thus

$$\bar{Z}_i = \frac{\frac{\partial Z}{\partial X}_i}{\left(\frac{\partial Z}{\partial X}\right)_{\max}} = \exp\left(\frac{-(2X_i)^2}{16 D_{AB} t_i}\right) \quad (C5)$$

Taking the natural logs of both sides of Eq. (C5) and rearranging yields

$$\frac{16 \ln(\bar{Z}_i)}{(2X_i)^2} t_i = - \frac{1}{D_{AB}} \quad (C6)$$

As in the multicomponent analysis, the imperfection of the interface must be compensated for by adding a zero time correction, t_o , to each experimental time. Adding this correction to Eq. (C6) and defining new variables

$$B_i = 16 \ln(\bar{Z}_i)/(2X_i)^2 \text{ and } \bar{D} = 1/D_{AB} \text{ gives}$$

$$B_i(t_i+t_o) = -\bar{D} \quad (C7)$$

The best values of D_{AB} and t_o may be found by defining the minimum of a variable Q which is defined as

$$Q = \sum_{i=1}^n [B_i(t_i+t_o) + \bar{D}]^2 \quad (C8)$$

where n is the total number of measurements. At the minimum of Q the partial derivatives with respect to t_o and \bar{D} go to zero, thus

$$\frac{\partial Q}{\partial t_o} = 2 \sum_{i=1}^n \{ [B_i(t_i+t_o) + \bar{D}] \cdot B_i \} = 0 \quad (C9)$$

$$\frac{\partial Q}{\partial \bar{D}} = 2 \sum_{i=1}^n [B_i(t_i+t_o) + \bar{D}] = 0 \quad (C10)$$

Rearranging Eqs. (C9) and (C10) gives

$$\sum_{i=1}^n [B_i] t_o + n \cdot \bar{D} = - \sum_{i=1}^n B_i t_i \quad (C11)$$

$$\sum_{i=1}^n [B_i^2] t_0 + \sum_{i=1}^n [B_i] \bar{D} = - \sum_{i=1}^n B_i^2 t_i \quad (C12)$$

Equations (C11) and (C12) are linear in t_0 and \bar{D} . The solutions to these equations are

$$D_{AB} = \frac{1}{\bar{D}} = \frac{\left[\sum_{i=1}^n B_i \right]^2 - n \sum_{i=1}^n B_i^2}{\left[\sum_{i=1}^n B_i^2 \right] \left[\sum_{i=1}^n B_i t_i \right] - \left[\sum_{i=1}^n B_i \right] \left[\sum_{i=1}^n B_i^2 t_i \right]} \quad (C13)$$

$$t_0 = \frac{n \sum_{i=1}^n B_i^2 t_i - \left[\sum_{i=1}^n B_i \right] \left[\sum_{i=1}^n B_i t_i \right]}{\left[\sum_{i=1}^n B_i \right]^2 - n \sum_{i=1}^n B_i^2} \quad (C14)$$

Thus the values of D_{AB} and t_0 may be determined directly from the experimental values of $2X_i$, Z_i , and t_i .

APPENDIX D

Least Square Analysis

In order to find the values of certain parameters which produced a minimum in an objective function, a technique called pattern search was used. This technique, which was first developed by Hooke and Jeeves (9), is useful in finding the maximum or minimum of a function of several variables.

The method is basically composed of two parts. The first part consists of local explorations in the vicinity of the base point. Each of the variables is perturbed by a small step, and the resulting change in the objective function is noted. If the step is an improvement, the next variable is treated in a similar manner. If not, a step is tried in the opposite direction. Only steps which improve the objective function are allowed.

After the local explorations have been completed, a pattern move is made. A pattern move consists of simultaneous changes in each of the variables depending upon the results of previous local exploration. The size of the pattern move may grow if repeated success in a particular direction is found.

If no improvements are found for a complete set of local explorations, the sizes of the steps are reduced. The search is terminated when the step sizes reach a pre-selected minimum.